

Evolutionary Optimization of High-Coverage Budgeted Classifiers

Nolan H. Hamilton

haminh16@wfu.edu

Department of Computer Science, Wake Forest University, Winston-Salem, NC, USA

Errin W. Fulp

fulp@wfu.edu

Department of Computer Science, Wake Forest University, Winston-Salem, NC, USA

Abstract

Classifiers are often utilized in time-constrained settings where labels must be assigned to inputs quickly. To address these scenarios, budgeted multi-stage classifiers (MSC) process inputs through a sequence of *partial* feature acquisition and evaluation steps with early-exit options until a confident prediction can be made. This allows for fast evaluation that can prevent expensive, unnecessary feature acquisition in time-critical instances. However, performance of MSCs is highly sensitive to several design aspects—making optimization of these systems an important but difficult problem.

To approximate an initially intractable combinatorial problem, current approaches to MSC configuration rely on well-behaved surrogate loss functions accounting for two primary objectives (processing cost, error). These approaches have proven useful in many scenarios but are limited by analytic constraints (convexity, smoothness, etc.) and do not manage additional performance objectives. Notably, such methods do not explicitly account for an important aspect of real-time detection systems—the ratio of “accepted” predictions satisfying some confidence criterion imposed by a risk-averse monitor.

This paper proposes a problem-specific genetic algorithm, *EMSCO*, that incorporates a terminal reject option for indecisive predictions and treats MSC design as an evolutionary optimization problem with distinct objectives (accuracy, cost, coverage). The algorithm’s design emphasizes Pareto efficiency while respecting a notion of aggregated performance via a unique scalarization. Experiments are conducted to demonstrate *EMSCO*’s ability to find global optima in a variety of $\Theta(k^n)$ solution spaces, and multiple experiments show *EMSCO* is competitive with alternative budgeted approaches.

Keywords

feature-budgeted classification, evolutionary computing, reject option, budgeted classification, resource-efficient learning

1 Introduction

Machine learning techniques have become popular among practitioners for deployment in real-time detection scenarios. However, traditional out-of-box methods are not always appropriate for resource-constrained contexts. Many application domains present implicit latency constraints between observation of inputs and label prediction, and a common difficulty regards balancing cost of processing with accuracy (Ji and Carin, 2007; Trapeznikov et al., 2013; Xu et al., 2012).

In these *budgeted* learning settings, the amount of resources expended while evaluating inputs represents the *cost of classification*. This cost is commonly specified further as the sum of *feature acquisition cost* and *classifier evaluation cost*. Feature acquisition refers to the process of

computing informative metrics for classification that are not present during the initial observation of inputs; Classifier evaluation cost is a measure of the resources spent evaluating an input with a classifier that has been trained on the acquired features. Note, cost of classification is often dominated by feature acquisition cost (Kusner et al., 2014; Xu et al., 2012).

For example, consider the task of classifying e-mail messages as spam. A large influx of messages must be evaluated quickly, and informative features such as number of URLs, subject-line character diversity, sender reputation score, etc. require CPU-time to compute. A classification scheme that requires a large set of such features for to label each input may therefore be impractical depending on the number of messages and desired processing speed. Fortunately, it is often possible to use smaller subsets of features to correctly classify a fraction of test-time inputs (Trapeznikov et al., 2013; Xu et al., 2012, 2014; Ji and Carin, 2007; Nan et al., 2016).

Multi-stage classifiers leverage this notion that some inputs may require only a few inexpensive features to be confidently labeled, while other “harder” inputs may require additional features for discernment. Using this design, a set of classifiers with growing feature sets are arranged in sequence to evaluate inputs (Trapeznikov et al., 2013; Ji and Carin, 2007; Wang et al., 2014). Once an input receives a confident class prediction, processing ceases and no cost is incurred for the remaining features that were not used. Specific use-cases of sequential, budgeted learning can be found across a diverse range of application domains (Dundar and Bi, 2007; Hamilton et al., 2020; Nogueira et al., 2019).

While budgeted learning schemes present an opportunity for efficient processing of inputs in time-critical instances, there are a multitude of important design considerations that can affect performance of these protocols, making configuration a difficult optimization problem. However, given the potential benefits, design of budgeted classifiers has become an active area of research in the past decade (Trapeznikov et al., 2013; Ji and Carin, 2007; Xu et al., 2014, 2012; Nan et al., 2016; Peter et al., 2017; Janisch et al., 2019).

1.1 Related Work

In this section, we offer a brief survey of prominent budgeted classification algorithms. Naturally, a common approach to optimizing budgeted classifiers involves constructing a surrogate loss function that penalizes error *and* cost of classification. This well-behaved loss function is then minimized with descent techniques.

(Ji and Carin, 2007) treats the problem as a partially-observable Markov process and requires estimation of class probability models that restrict applicability in some use cases. (Trapeznikov et al., 2013) formulates the problem with reject options at each stage comprised of weak learners. These reject classifiers are optimized using coordinate descent on a feature-budgeted empirical risk function. To avoid difficult combinatorial aspects, the order of features is fixed beforehand. The result is a solution with guaranteed local optimality—but only with respect to the chosen ordering of features and stages. (Wang et al., 2014) establishes an improvement over the myopic approach proposed in (Trapeznikov et al., 2013) by devising a convex loss function. The authors are then able to guarantee globally optimal solutions within the context of their formulation and a fixed feature/stage order.

While many budgeted protocols rely on a fixed stage design, several existing methods incorporate feature selection/order implicitly. (Xu et al., 2012) proposes *GreedyMiser*—a feature-budgeted variant of stage-wise regression (Friedman, 2001). Limited-depth regression trees are used as weak learners and are constructed with a modified impurity function accounting for cost of feature extraction. These weak learners are combined to form a final classifier. For its relative simplicity and good scaling to high-dimensional data, *GreedyMiser* has become one of the most popular and best-cited feature-budgeted approaches to classification. (Xu et al., 2014) proposes *Cost-Sensitive Tree of Classifiers*; This method builds a tree of classifiers optimized for a

specific subset of the input space. The input space is partitioned based on classifier predictions. Classifiers that reside deep in the tree become “experts” for a small subset of the input space, and intermediate classifiers determine the path of instances through the tree. CSTC is trained with a single global loss function, where the test-time cost penalty is a relaxation of the expected cost.

While the described methods provide a pathway to efficient classification of inputs in resource-constrained settings and significant theoretical guarantees, several limitations are consistent throughout this body of work. First, many of the methods do not optimize the order of the features/stages (Trapeznikov et al., 2013; Wang et al., 2014) and instead resort to heuristics to choose an ordering such as increasing cost (expensive features placed at later stages). This can be inefficient if many cheap features are uninformative. Additionally, intuitively modeling complex feature interactions beforehand can prove difficult, and such interactions may be consequential if variables are more/less discriminative when grouped together (Ji and Carin, 2007).

Furthermore, these methods rely on a single homogeneous loss function that can fail to properly manage multiple objectives in a fitness landscape that is not well-behaved. This can be problematic in scenarios where important non-dominated solutions are not supported by scalarization and several objectives are consequential (Deb, 2001; Boyd and Vandenberghe, 2004). Indeed, there are important performance aspects beyond cost and accuracy in real-time prediction systems, and one frequently neglected metric is *conclusiveness*—the ratio of predictions deemed sufficiently confident to be recorded and not discarded by a terminal *reject option*. This metric is also referred to as “coverage”¹ in the domain of selective classification (SC) (El-Yaniv and Wiener, 2010; Geifman and El-Yaniv, 2017). With this in mind, the cost/accuracy framework embraced by alternative methods is potentially limiting, and a need arises for a budgeted approach with a terminal reject option that can effectively manage several objectives explicitly.

Note, there are several loosely related learning paradigms that will not be addressed in this manuscript. *Classifier cascades*, for example, leverage an assumption of class imbalance and are restricted to binary classification (Viola and Jones, 2001). *Budgeted feature selection* techniques (Yu et al., 2020) aim to identify a cheap subset of features to accurately classify inputs but make an assumption that certain features are not relevant for *any* inputs and discard them entirely.

1.2 Evolutionary Approaches to Multi-Stage Classifier Design

Many of the issues discussed above can be alleviated by formulating MSC design in a way that incorporates a terminal reject option, considers order/composition of stages, and manages multiple objectives in a Pareto efficient manner. This paper builds on a preliminary approach² (Hamilton and Fulp, 2020) of the authors to treat multi-stage classifier configuration as a combinatorial optimization problem to be solved with evolutionary algorithms (EAs). EAs employ a population-based approach to optimization in which the generation/population G_1 is a product of mutation, selection, and crossover on the solutions in G_0 . These algorithms possess desirable properties in the setting of multi-objective optimization (Deb, 2001) when gradients are not available and mathematical flexibility is needed.

Three objectives are considered: conclusive accuracy, feature acquisition cost, and conclusiveness (See Section 2.2 for a detailed description of these objectives.) Leveraging the flexibility of EAs, EMSCO is unique compared to alternative budgeted approaches in that it defines these objectives with indicators. This allows for a natural treatment of the problem that is less dependent on approximation. Additionally, by incorporating non-domination level in the fitness

¹In this manuscript, we use the terms “coverage” and “conclusiveness” interchangeably.

²In contrast to the method proposed in this paper, the preliminary approach uses generic evolutionary operators, a less robust elitism procedure, and does not provide any theoretical guarantees.

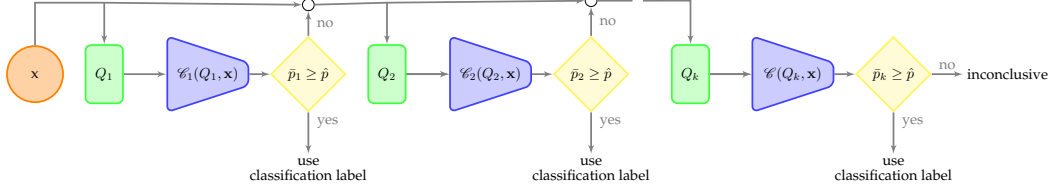


Figure 1: Design of a k -stage classifier with confidence threshold \hat{p} . Inputs are processed sequentially through classification stages until they achieve a class probability greater than \hat{p} or all features have been exhausted.

function and applying domain-specific knowledge in the evolutionary operators, EMSCO ensures several important properties described later (Section 3.3).

2 A Formal Description of Multi-Stage Classification

This section details the setting in which EMSCO is deployed. See Table 1 for a description of notation and symbols used throughout the paper and Figure 1 for a visual depiction of EMSCO’s workflow.

Assume a classification scenario in which inputs are evaluated with a potential feature set \mathcal{F} , where $|\mathcal{F}| = n$. Upon initial observation, an input $\mathbf{x} \in \mathcal{X}_{test}$ begins with no acquired features, and features are thereafter attained sequentially through stages. That is, stage j acquires a subset of features $Q_j \subseteq \mathcal{F}$ to evaluate³ input \mathbf{x} . The stage- j classifier $\mathcal{C}(Q_j, \mathbf{x})$, learned on features in Q_j during training-time, returns a set of prediction confidences $\mathcal{P}_{\mathbf{x}_j} = \{p_1, p_2, \dots, p_l\}$ corresponding to l possible labels for the input. Note, every feature has a corresponding cost of acquisition given by the set \mathcal{C} —acquiring feature \mathcal{F}_i for evaluation of \mathbf{x} increases the classification cost of \mathbf{x} by \mathcal{C}_i . After a particular feature has been acquired for an input in stage j , it can be referenced in stage $j + 1, j + 2, \dots, k$ for no cost.

We assume a *risk-averse monitor* has decided to accept only confident predictions. At preterminal stages $j < k$, a reject decision is made to determine whether the input prediction is sufficiently confident to be accepted or if additional processing is necessary (in which case, we say \mathbf{x} has been “rejected” to the next stage). Let $\bar{p}_j = \max \mathcal{P}_{\mathbf{x}_j}$ and \hat{p} be a confidence threshold specified by the monitor. At stage $j < k$, if $\bar{p}_j < \hat{p}$, the input is sent to stage $j + 1$ where it is evaluated with feature set Q_{j+1} (Note, $Q_j \subset Q_{j+1}$). Conversely, if $\bar{p}_j \geq \hat{p}$, processing ceases, and \mathbf{x} is assigned the label corresponding to the maximum class probability.

At the terminal stage k , if $\bar{p}_k < \hat{p}$, evaluation of \mathbf{x} is deemed *inconclusive* with no label assigned. In this case, we say that \mathbf{x} has been *terminally rejected*. This is a safe but generally undesirable result as it decreases utility of the system—while desiring at least \hat{p} accuracy, the above-mentioned risk-averse monitor also desires that the system yield insight. Figure 2 depicts the effect of \hat{p} on system performance in a generic⁴ setting.

With a confidence threshold specified *a priori* via cost/benefit analysis, our aim is to find a sequence of stages that provides high accuracy (at least \hat{p}), low processing cost, and high coverage. See Section 2.3 for the formal problem statement.

³The stage $\mathcal{C}(Q_j, \mathbf{x})$ can use any classification algorithm suitable for the given context. For the sake of generalization and computational efficiency, EMSCO employs ℓ_2 -regularized logistic regression at each stage in this paper.

⁴Objectives were measured using a cost-ordered two-stage model. We used Scikit-Learn’s (Pedregosa et al., 2011) function `make_classification()` to generate a synthetic data set with fifteen features, five-hundred samples, and binary labels. Feature costs were determined as a positive linear function of feature importance as determined by Gini impurity.

| Symbol | Description |
|--------------------------------|---|
| β | stage count bias parameter |
| b | elitism proportion |
| \mathcal{C} | feature costs |
| $\mathcal{C}(Q_j, \mathbf{x})$ | returns class probabilities for \mathbf{x} after j^{th} stage evaluation |
| E_0^* | unique non-dominated solutions in a given generation |
| $\mathcal{E}(g_1, g_2, g_3)$ | objective Euclidean norm |
| \mathcal{F} | feature set |
| G_h | refers to the h^{th} generation |
| $\ G\ $ | population size |
| g | convergence parameter |
| k | max number of stages |
| M | elite population size (unfixed) |
| \hat{m} | mutation rate |
| n | number of features |
| N | number of test records |
| $\mathcal{N}(G_h)$ | returns the non-dominated front in generation G_h |
| $\mathcal{P}_{(n,j)}$ | ordered j -partitions of \mathcal{F} |
| \bar{p}_j | maximum class probability after j^{th} stage |
| \hat{p} | confidence threshold |
| $\ Q\ $ | stage count of solution Q |
| Q_j | features in stage j |
| $[Q]$ | chromosome representation of Solution Q |
| $[Q]_i$ | stage assignment for feature i |
| \hat{r} | recombination rate |
| r_{max} | rank of the non-dominated solutions in a specified population |
| $\mathcal{S}_{(n,k)}$ | all solutions with at most k stages |
| T_i | cost class of i^{th} feature |
| $\lceil \cdot \rceil$ | returns next smallest integer |
| $\mathbb{1}[\cdot]$ | indicator function |
| \succ | Pareto dominance relation |

Table 1: Notation and Symbols used in Manuscript

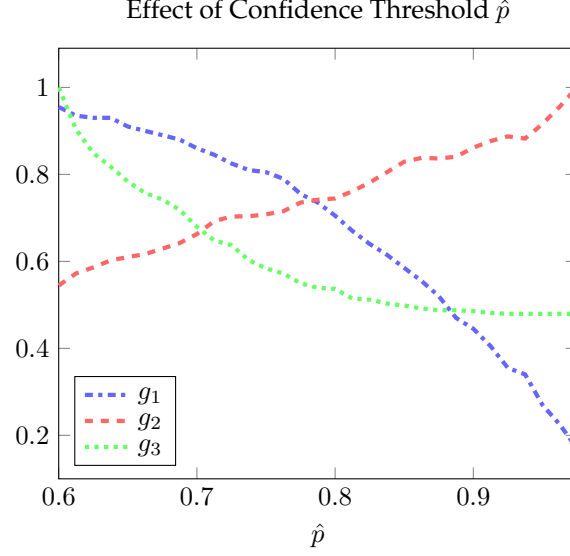


Figure 2: Example system behavior under varying \hat{p} . Higher \hat{p} corresponds to greater conclusive accuracy but lower utility and increased cost.

2.1 Solution Space

To provide insight into the nature and difficulty of the problem under our formulation, we offer an analysis of the solution space. Solutions are k -partitions of the feature set \mathcal{F} . That is,

$$\bigcup_{j=1}^{j=k} Q_j = \mathcal{F}$$

where $Q_j \neq \emptyset$ denotes the new features acquired in stage j . The order of the stages is also considered. For example, if $\mathcal{F} = \{\mathcal{F}_1, \mathcal{F}_2, \mathcal{F}_3, \mathcal{F}_4\}$, then

$$Q = \{\{\mathcal{F}_1, \mathcal{F}_2\}, \{\mathcal{F}_3, \mathcal{F}_4\}\} \neq \{\{\mathcal{F}_3, \mathcal{F}_4\}, \{\mathcal{F}_1, \mathcal{F}_2\}\}$$

The number of ordered k -partitions, $\mathcal{P}_{(n,k)}$, on a feature set with dimension n is then computed by multiplying the number of unordered partitions by $k!$:

$$||\mathcal{P}_{(n,k)}|| = k! \cdot S_2(n, k) = \sum_{i=0}^k (-1)^{k-i} \binom{k}{i} i^n, \quad (1)$$

where $S_2(n, k)$ represents the number of unordered k -partitions of a set with n elements, also known as a *Stirling number of the second kind* (Knuth, 1998). In practice, EMSCO treats k as an upper bound for stage count—the search space, $\mathcal{S}_{(n,k)}$, is the set of all solutions with *up to and including* k stages. That is,

$$\mathcal{S}_{(n,k)} = \bigcup_{j=1}^{j=k} \mathcal{P}_{(n,j)}. \quad (2)$$

The following theorem gives the limiting behaviour of this solution space.

Theorem 1. For a fixed k such that $k \leq n$, the number of candidate solutions $||\mathcal{S}_{(n,k)}||$ is asymptotically equivalent to k^n .

Proof. We first show that the ratio of quantities $||\mathcal{P}_{(n,k)}||$ and k^n approaches one as $n \rightarrow \infty$. Since k is fixed, every term in right-hand-side of the expression below approaches zero except the last.

$$\lim_{n \rightarrow \infty} \frac{1}{k^n} \sum_{i=0}^k (-1)^{k-i} \binom{k}{i} i^n = \lim_{n \rightarrow \infty} \pm \frac{\binom{k}{0} 0^n}{k^n} \pm \frac{\binom{k}{2} 2^n}{k^n} \pm \dots + \frac{\binom{k}{k} k^n}{k^n},$$

where $\frac{\binom{k}{k} k^n}{k^n} = 1$. Thus, $\mathcal{P}_{(n,k)} \sim k^n$. Since there is no intersection between terms in the union on the RHS of Equation 2,

$$\sum_{j=1}^{j=k} ||\mathcal{P}_{(n,j)}|| = ||\mathcal{S}_{(n,k)}||.$$

Using this fact and $||\mathcal{P}_{(n,j)}|| \sim j^n$, we can quickly show:

$$\lim_{n \rightarrow \infty} ||\mathcal{S}_{(n,k)}|| = \lim_{n \rightarrow \infty} \frac{1}{k^n} \sum_{j=1}^{j=k} ||\mathcal{P}_{(n,j)}|| = \lim_{n \rightarrow \infty} \frac{1}{k^n} \sum_{j=1}^{j=k} j^n = \lim_{n \rightarrow \infty} \left(\frac{k}{k}\right)^n = 1.$$

That is, $||\mathcal{S}_{(n,k)}|| \sim k^n$. □

In practice, all features in stage j are automatically appended to stage $j + 1$ as they are already acquired and can be referenced for no cost. However, this technicality does not affect the above analysis, since it depends only on the unique elements acquired at each stage.

As our defining structure for MSCs, ordered feature set partitions possess several beneficial properties. In many cases, certain features are uninformative alone but become highly discriminative when evaluated together (Ji and Carin, 2007). By allowing stages to contain multiple features, these scenarios are acknowledged implicitly during optimization. Additionally, using the representation proposed in Section 3.1, ordered feature set partitions can be conveniently modeled as chromosomes. Notice that \hat{p} is fixed since it is assumed this value is set *a priori* by a risk-averse monitor whose misclassification penalties warrant such a threshold.

2.2 Objectives

Objectives are designed to incorporate important performance aspects of a real-time detection system. Leveraging the mathematical flexibility of EAs, we can incorporate pathological functions (e.g., indicators) and define several objectives separately. All objectives are to be *maximized* in the range $[0, 1]$. See Figure 3 for an example visual depiction of the fitness landscape determined by these objectives. In the following subsections, m denotes the index of the final stage at which input \mathbf{x} is processed.

2.2.1 Conclusiveness

This objective attempts to quantify an abstract notion of *utility* representing the insight provided by the classification system under a minimum confidence constraint. Specifically, conclusiveness is measured as the fraction of predictions that meet a targeted confidence threshold, \hat{p} .

$$g_1(Q) = \frac{1}{N} \sum_{\mathbf{x} \in \mathcal{X}_{test}} \mathbb{1}[p_m^- \geq \hat{p}] \quad (3)$$

If conclusiveness is not considered as an objective, then a risk-averse monitor accepting only confident predictions may obtain little information from the system. Such a monitor wishes

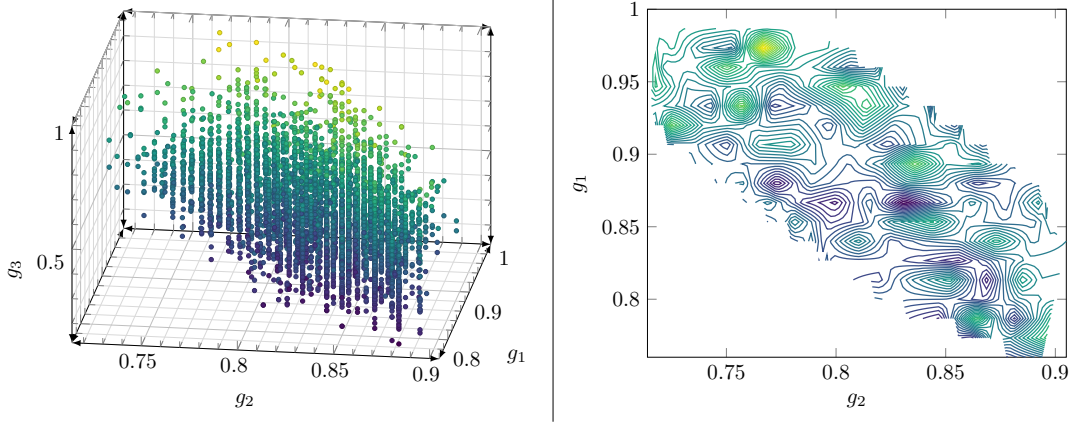


Figure 3: Scatter plot (left) and contour map (right) of a random sample of (g_1, g_2, g_3) for five-thousand $Q \in \mathcal{S}_{(12,3)}$ on the Heart Failure Clinical Records data set ($\hat{p} = 0.75$). The color in both plots is determined by g_3 , where darker color corresponds to low g_3 (high cost). Note the trade-off between conclusive accuracy and cost: g_3 is relatively low in the bottom-right corner of the contour plot and relatively high in the top-left corner.

to be correct at a rate at least \hat{p} but also desires that the classification system yield sufficient information and not terminally reject an excessive fraction of predictions in order to achieve sufficient accuracy.

Such confidence-constrained classification is common in practice (Lichtblau and Stoean, 2019; Patel et al., 2019). Despite being an important aspect of performance that has presence in the literature outside of budgeted learning (Cortes et al., 2016; Geifman and El-Yaniv, 2017), conclusiveness (coverage) is not accounted for explicitly in current budgeted learning methods, to the best of our knowledge. Note that reject decisions can be defined in a number of ways (El-Yaniv and Wiener, 2010; Geifman and El-Yaniv, 2017). *EMSCO* utilizes a rejection protocol based on confidence thresholds because it is computationally efficient and frequently used in practice. It is also intuitive; when a well-calibrated classification algorithm (e.g., logistic regression) is used at each stage, a reject protocol based on confidence thresholds may effectively ensure accuracy above \hat{p} (Figure 2). Note, however, poorly *calibrated* classification algorithms (i.e., those with large disparities between confidence scores and actual class probabilities) may obscure the interpretation of this rejection protocol (Kuhn et al., 2013).

2.2.2 Conclusive Accuracy

Conclusive accuracy is the proportion of conclusive, correctly classified inputs with respect to the total number of conclusive predictions. Let y denote the true label for $\mathbf{x} \in \mathcal{X}_{test}$, and $\bar{\mathcal{C}}_m(Q_m, \mathbf{x})$ return the label corresponding to the maximum class probability after evaluation in stage m . Conclusive accuracy is defined as:

$$g_2(Q) = \frac{1}{N^*} \sum_{\mathbf{x} \in \mathcal{X}_{test}} \mathbb{1}[\bar{\mathcal{C}}_m(Q_m, \mathbf{x}) = y \ \& \ \bar{p}_m \geq \hat{p}], \quad (4)$$

where N^* denotes the number of conclusive predictions. By default, g_2 applies the same penalty for all misclassification types. However, it can be easily modified to penalize different cases (e.g., false negative, false positive) with a piecewise function.

2.2.3 Cost

Because feature acquisition typically comprises the bulk of test-time processing expense (Kusner et al., 2014), raw cost $g_3^*(\cdot)$ is measured as the *average sum of acquisition costs per test input*:

$$g_3^*(Q) = \frac{1}{N} \sum_{\mathbf{x} \in \mathcal{X}_{test}} \left(\sum_{j=1}^{j=m} c_{Q_j} \right)$$

where c_{Q_j} denotes the sum of features' costs in stage j . Note that the cost of inconclusive records is considered since the system requires resources to arrive at an inconclusive result.

To maintain consistency as a maximization problem and a $[0,1]$ scale for objectives, the minimum raw cost of all solutions in the current generation is determined and used for normalization. Then, for $Q \in G_h$, inverse cost $g_3(Q)$, is measured as:

$$g_3(Q) = \frac{\min_{U \in G_h} g_3^*(U)}{g_3^*(Q)} \quad (5)$$

2.3 Problem Definition

EMSCO seeks an ordered feature set partition, $Q \in \mathcal{S}_{(n,k)}$, to maximize objectives g_1, g_2, g_3 through the perspective of *Pareto efficiency*. Consider two chromosomes Q_A, Q_B . If every $g_i(Q_A) \geq g_i(Q_B)$, and there is at least one objective such that $g_i(Q_A) > g_i(Q_B)$, then Q_A is said to *dominate* Q_B , and this relationship is denoted as $Q_A \succ Q_B$. A solution that is not dominated by any solution in an arbitrary population G is said to be *non-dominated* and solves its respective multi-objective optimization problem (Deb, 2001). Note, $\mathcal{N}(G)$ returns the set of all non-dominated solutions in G , and this set of non-dominated solutions is referred to as the *Pareto frontier* of population G .

EMSCO addresses the following multi-objective optimization by seeking solutions that are non-dominated with respect to $\mathcal{S}_{(n,k)}$:

$$\arg \max_{Q \in \mathcal{S}_{(n,k)}} (g_1(Q), g_2(Q), g_3(Q)). \quad (6)$$

In this manuscript, solutions to this problem are referred to as *globally Pareto optimal* or *globally non-dominated*.

3 Evolving Multi-Stage Classifier Configurations

This manuscript proposes a problem-specific evolutionary algorithm, *Evolutionary Multi-Stage Classifier Optimizer* (EMSCO), that seeks to solve the optimization problem in (6). EMSO evolves improved populations of configurations over a series of generations (iterations of the algorithm). Key aspects of EMSO include the chromosomal representation of solutions and the evolutionary operators employed to create new populations. These are detailed in the sections below.

3.1 Chromosome Representation of Ordered Feature Set Partitions

Ordered feature set partitions can be conveniently represented as lists. Let Q be a solution in $\mathcal{S}_{(n,k)}$. Then the chromosomal representation of Q is:

$$[Q] \in \{0, 1, \dots, k-1\}^n,$$

where $[Q]_j$ corresponds to the j th feature's stage assignment. Note, to maintain consistency with array notation, the elements in $[Q]$ are *zero-indexed*; so $[Q]_j = s$ assigns feature j to stage

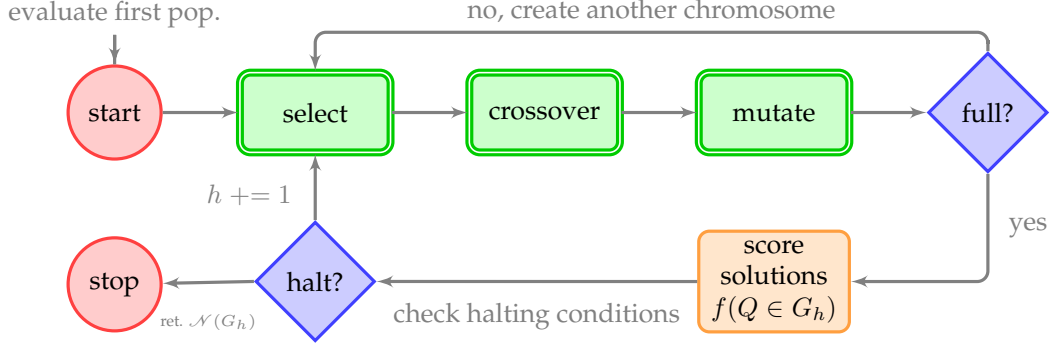


Figure 4: Flow chart of the tasks used for identifying MSC configurations. Double-lined blocks (in green) contain traditional GA processes, while the orange block performs MSC configuration assessment (ranking and fitness).

$s + 1$. For example, given the ordered set partition $Q = \{\{\mathcal{F}_1, \mathcal{F}_2\}, \{\mathcal{F}_3, \mathcal{F}_4\}\}$, the corresponding list representation would be $[Q] = \{0, 0, 1, 1\}$.

3.1.1 Stage Compression

Note that there is not an exact correspondence between list representations and ordered feature set partitions. For example, $\{0, 0, 0, 2\} \in \{0, 1, 2\}^4$, but since stage two is empty, this list does not correspond to an ordered feature set partition and is not a feasible solution. Asymptotically, the disparity between these sets becomes less problematic (Theorem 1), but a remedy is still needed for low dimension data sets.

After a new solution is generated, it is checked for gaps with the function, $gaps([C])$, that returns true if any $j = 0 \dots \|C\| - 1$ is missing. If any such gaps exist, the solution is modified with $compress([C])$ to redefine stage assignments in the following manner: For any missing $j^* \in \{0, \dots, \|C\| - 1\}$, iterate through $[C]$ and replace $j^* + 1$ with j^* . For instance, in the above example, $\{0, 0, 0, 2\}$ would be compressed to $\{0, 0, 0, 1\}$.

3.2 Evolutionary Processes

EMSCO's evolutionary operators are designed to leverage problem-specific knowledge while maintaining breadth of search to avoid premature convergence. These operators are applied in sequence to form a new population per generation. Note, in the following subsections, \hat{m} denotes the probability of mutation, and \hat{r} denotes the probability of recombination.

3.2.1 Selection

Selection is the process in which individual solutions (chromosomes) are chosen from a population for the recombination stage. EMSCO utilizes roulette wheel selection (Eiben and Smith, 2015), which biases the selection with respect to the fitness metric (described in Section 3.3). As a result, more fit chromosomes are more likely to be chosen.

3.2.2 Elitism

The elitism protocol applied in this paper is designed to preserve all *unique* non-dominated solutions to the subsequent generation. Let E_0^* denote the set of unique non-dominated chromosomes within generation G_h , and let G_h^* denote the set of unique solutions in generation G_h . For elitism parameter b in the open interval $(0, 1)$, the top $M = \max(\lceil b \|G_h^*\rceil, \|E_0^*\|)$ solutions in each generation are sent to the subsequent generation without modification. As a halting

condition, if $M \geq \|G\|$, EMSCO returns the entire elite population and stops execution. This helps ensure the algorithm does not discard non-dominated solutions (See Section 3.4).

3.2.3 Mutation

In general, mutation operators are used to maintain genetic diversity from one generation's population of chromosomes to the next (Eiben and Smith, 2015). EMSCO uses mutation to implement this behavior while also addressing certain domain-specific concerns.

If performance is comparable between solutions $Q_A, Q_B \in G_h$, the solution with lower stage count is preferred as it will likely impose fewer classifier evaluation costs than the alternative, and these costs can prove consequential in high-dimensional settings or when expensive classification algorithms are employed at each stage (Artières et al., 2016). Moreover, in marginal cases, each additional stage in an MSC presents another opportunity to trigger a wrong but conclusive prediction. An incorrect prediction only needs to be declared conclusive once in order to be recorded definitively (Section 2), and the probability of this event may increase as more trials (stages) are introduced.

With these aspects in mind, we prefer that solutions with high stage count not be considered until lower stage counts have proven to be insufficient in comparison. To this end, a discrete, monotonically decreasing probability distribution is desired to mutate chromosomes' stage assignments. The beta-binomial distribution (Casella and Berger, 2001) with $\alpha = 1$ & $\beta > \alpha$, denoted $BB(\alpha = 1, \beta)$, satisfies this criteria and possesses several convenient properties for adjusting bias of the mutation operator towards low stage assignments. Let $0 \leq j \leq \|Q\|$ be a potential stage assignment for the i^{th} feature in chromosome Q . The probability mass function is given by:

$$\mathbb{P} [[Q]_i \leftarrow j] = \binom{\|Q\|}{j} \frac{B(j+1, \|Q\| - j + \beta)}{B(1, \beta)} \quad (7)$$

where $B(\cdot)$ denotes the beta function. For a chromosome with stage count $\|Q\|$, this distribution has an expected value $(\frac{\|Q\|}{\beta+1})$ that is decreasing with respect to β . This parameter can therefore be used to adjust bias, where greater β corresponds to greater preference for low stage assignments.

Despite the bias described above, it is important that the mutation operator allows creation of new stages when warranted—in certain scenarios (e.g., high n), a low stage count may yield high feature acquisition cost. The mutation operator creates new stages in $[Q]$ by assigning stage $\|Q\|$ to one of the elements⁵, and the probability of adding a stage in this manner can be controlled by increasing/decreasing β . See Algorithm 1 for a pseudo-code representation of the mutation procedure.

The condition $\text{count}([Q]_i, [Q]) > 1$ checks if there is more than one occurrence of $[Q]_i$ in $[Q]$ and is considered to ensure that mutation will not result in an empty stage. The draw from $\min(\|Q\|, k-1)$ elements ensures that the maximum number of stages k is not exceeded.

3.2.4 Recombination

EMSCO's recombination/crossover operator takes into account the differing contexts of stage assignments within the parent solutions. To implement crossover, two parent chromosomes, $P_A, P_B \in G_h$ are selected according to the protocol described in Section 3.2.1. With probability \hat{r} , these solutions are then combined to produce a child solution, $C \in G_{h+1}$. With probability $1 - \hat{r}$, recombination/crossover returns one of P_A, P_B via a uniform random selection (coin flip).

⁵Recall, the list representation is zero-indexed at each element, so a stage assignment of $\|Q\|$ sends the feature to new stage $\|Q\| + 1$

Algorithm 1: Mutation

```
 $Q$  is a new chromosome  
//  $0 \leq i < n$   
; for each  $i^{\text{th}}$  feature do  
| if ( $\text{rand}([0, 1]) \leq \hat{m}$  &  $\text{count}([Q]_i, [Q]) > 1$ ) then  
| |  $[Q]_i \sim \text{BB}(\min(\|Q\|, k - 1), 1, \beta)$ ;  
| end  
end
```

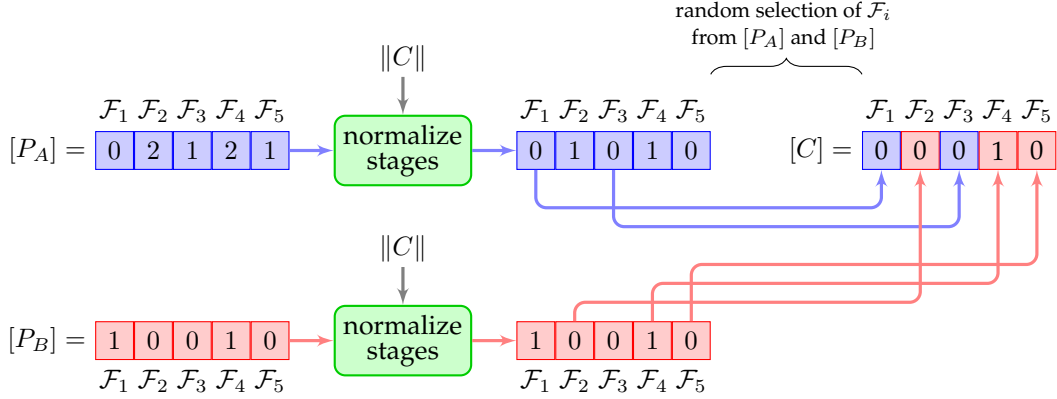


Figure 5: Example stage normalization and recombination, where $[P_A]$ and $[P_B]$ are parents and $[C]$ is the child. In this example, the child’s stage count is selected as $\|P_B\|$.

The first step in recombination of P_A and P_B chooses a stage count for the child solution. Three options exist for $\|C\|$: $\|P_A\|$, $\|P_B\|$, $\left\lfloor \frac{\|P_A\| + \|P_B\|}{2} \right\rfloor$, where the third option is incorporated to facilitate consideration of solutions with intermediate stage counts and introduce a notion of blending parent chromosomes with respect to stage count. After a stage count is decided, each of the child’s features must be assigned a stage. Each i th assignment is initially chosen to be either $[P_A]_i$ or $[P_B]_i$. Let $R \in \{P_A, P_B\}$ denote the parent corresponding to this choice. In an *attempt* to maintain the context of the parent’s stage assignment for the i th feature, the initial selection $[R]_i$ is normalized according to $\|R\|$ to acquire the relative order of the stage assignment within R . This ratio is then multiplied by $\|C\|$, rounded, and decremented to obtain a zero-indexed, approximate analog of $[R]_i$ in $[C]$. Alternatively, if raw values were assigned ($[C]_i \leftarrow [R]_i$), then the chosen stage assignment may lose context in the child solution’s structure. Consider, for example, the role of the second stage in a five-stage system versus the role of the second stage in a two stage system. In the latter case, the second stage provides the final evaluation of inputs; In the former case, the second stage is an early evaluation. The recombination process is detailed in Algorithm 2.

3.3 Evaluating Chromosomes

For a solution $Q \in G_h$, fitness computed using the ℓ_2 norm of $\{g_1(Q), g_2(Q), g_3(Q)\}$, denoted by $\mathcal{E}(Q)$, and an exponential term accounting for the *Pareto rank* of Q with respect to the current generation. In this paper, Pareto rank, or *non-domination level* (Deb et al., 2002), is an indication of the solution’s performance from the perspective of Pareto efficiency. This mixed formulation

Algorithm 2: Recombination

```
[PA], [PB] are parents selected for recombination in Gh
Initiate child [C] ← [0, 0, ..., 0]
||C|| ← rand { ⌊  $\frac{\|P_A\| + \|P_B\|}{2}$  ⌋, ||PA||, ||PB|| };
// 0 ≤ i < n
for each ith feature do
    R = rand {PA, PB};
    Assign stage to the ith feature of the child
    [C]i ← round (  $\frac{[R]_{i+1}}{\|R\|}$  ) ||C||;
    [C]i ← [C]i - 1;
    [C]i ← max ([C]i, 0);
end
return [C]
```

of fitness intends to respects Pareto efficiency and raw aggregated performance simultaneously.

3.3.1 Pareto Rank of Chromosomes

To compute $rank(Q)$ in generation G_h , we first determine the non-dominated solutions in G_h . This set of solutions E_0 is then removed from G_h . The non-dominated solutions in set $G_h \setminus E_0$ are then stored in the set E_1 . This process of removing non-dominated solutions continues so that E_t contains the non-dominated solutions in the population $G_h \setminus E_0 \setminus E_1 \setminus \dots \setminus E_{t-1}$. Once all solutions have been assigned to some E_t , the ranking procedure is finished. Let E_{t^*} denote the final non-dominated set removed from G_h , and let $Q \in E_t$. Then

$$rank(Q) = t^* - t \quad (8)$$

Let $R, Q \in G_h$ be chromosomes in the h^{th} generation. $rank(R) > rank(Q)$ does not necessarily imply $R \succ Q$ —it only implies that there exists some chromosome $S \in G_h$ such that $S \succ Q$ and $S \not\succ R$. Note that our assignment of non-domination level is flipped—typically, the first non-dominated set is assigned zero rank (Deb et al., 2002). However, we define $rank(\cdot)$ so that the initial (best) set of non-dominated solutions is assigned the greatest value. The motivation for this may become clearer in the next subsection, where we define fitness.

3.3.2 Fitness Function

Fitness of chromosome Q is computed as a product involving $rank(Q)$ and the ℓ_2 norm, $\mathcal{E}(Q)$. Let $l_{\mathcal{E}}$ and $u_{\mathcal{E}}$ denote the minimum and maximum values of $\mathcal{E}(\cdot)$ in generation G_h , respectively. For some $\epsilon > 0$, we set

$$\gamma = \frac{u_{\mathcal{E}}}{l_{\mathcal{E}}} + \epsilon.$$

Fitness is defined as:

$$f(Q) = \gamma^{rank(Q)} \sqrt{g_1(Q)^2 + g_2(Q)^2 + g_3(Q)^2}, \quad (9)$$

By default, EMSCO uses $\epsilon = 0.01$, but this value can be modified to any positive real value. Rather than use a linear weighted-sum, the ℓ_2 norm is incorporated for its stability and to introduce a visual interpretation of aggregated performance as distance from the origin. This formulation of fitness contributes to several useful properties of EMSCO discussed in the next

section. Note, the global *scalarized* optimization problem posed by this fitness function is:

$$\arg \max_{Q \in \mathcal{S}_{(n,k)}} f(g_1(Q), g_2(Q), g_3(Q)) \quad (10)$$

3.4 Algorithmic Details and Guarantees

EMSCO begins by generating a random initial population of $\|G\|$ chromosomes by calling the function *init()*, which creates solutions by applying the mutation operator to the default one-stage solution $([0, 0, \dots, 0])$. After the first population has been generated, the main loop begins. Three halting conditions are checked before each iteration by calling the function, *converged()*, which returns true if any of the following conditions are satisfied: (i) the maximum number of iterations (*max_iter*) has been executed, (ii) the number of unique non-dominated solutions exceeds the specified population size, or (iii) the highest-scoring chromosome has remained constant for the past g generations. If none of these halting conditions is true, the loop proceeds, and the next population of solutions is produced using elitism, selection, recombination, and mutation as described in Section 3.2. When the loop ends, the list of all non-dominated solutions in the final generation is returned, sorted by fitness. Note that EMSCO may return

Algorithm 3: EMSCO

```

 $G_0 \leftarrow \text{init}();$ 
 $h \leftarrow 0$ 
while not converged() do
     $\text{rank}(G_h); \text{sort}(G_h, \text{key} = f(\cdot));$ 
     $\text{elite\_size} \leftarrow \max(\lceil b \|G_h^*\| \rceil, \|E_0^*\|);$ 
     $\text{elite\_pop} \leftarrow G_h[0 : \text{elite\_size}];$ 
     $G_{h+1} \leftarrow \text{append}(\text{elite\_pop});$ 
    while  $\|G_{h+1}\| < \text{pop\_size}$  do
         $P_A, P_B \leftarrow \text{select}();$ 
         $[C] \leftarrow \text{recombine}([P_A], [P_B]);$ 
         $[C] \leftarrow \text{mutate}([C]);$ 
         $G_h \leftarrow \text{append}(C);$ 
    end
     $h \leftarrow h + 1;$ 
end
return  $\mathcal{N}(G_h);$ 

```

$M > \|G\|$ chromosomes at the final generation when the number of unique non-dominated solutions exceeds the population size. Several important properties of EMSCO follow as consequences of the design aspects described heretofore.

Property 1. *EMSCO preserves globally non-dominated solutions and returns them at the terminal generation.*

Proof. Suppose for contradiction that some globally non-dominated chromosome D was initially encountered in G_h but not returned at terminal generation G_{term} . That is, $D \in G_h$ and $D \notin \mathcal{N}(G_{\text{term}})$.

As a consequence of the elitism protocol and halting conditions of EMSCO, D must have been dominated in some population $G_h, G_{h+1}, \dots, G_{\text{term}}$ to have been discarded. This contradicts our initial supposition, since a globally non-dominated solution in $\mathcal{S}_{(n,k)}$ will likewise be non-dominated in any *subset* of $\mathcal{S}_{(n,k)}$. \square

Property 2. Let $Q \in G_h$. (i) Probability of selection is strictly increasing with respect to $\text{rank}(Q)$, and, (ii) within a particular rank, probability of selection is strictly increasing with respect to $\mathcal{E}(Q)$.

Proof.

(i) Let R_A, R_B be chromosomes in generation G_h such that

$$r_B = \text{rank}(R_B) > r_A = \text{rank}(R_A).$$

Because $\frac{u_{\mathcal{E}}}{l_{\mathcal{E}}}$ maximizes the ratio between any two $\mathcal{E}(R_A)$ and $\mathcal{E}(R_B)$, and we have assumed $r_B > r_A$, we have that

$$\left(\frac{u_{\mathcal{E}}}{l_{\mathcal{E}}} + \epsilon\right)^{r_B - r_A} > \frac{\mathcal{E}(R_A)}{\mathcal{E}(R_B)},$$

since γ^r is strictly increasing with respect to γ and r . The above inequality is equivalent to

$$\left(\frac{u_{\mathcal{E}}}{l_{\mathcal{E}}} + \epsilon\right)^{r_A} \mathcal{E}(R_A) < \left(\frac{u_{\mathcal{E}}}{l_{\mathcal{E}}} + \epsilon\right)^{r_B} \mathcal{E}(R_B)$$

which, by definition, implies

$$f(R_A) < f(R_B).$$

The result follows from the use of roulette wheel selection.

(ii). If $r_A = r_B$, fitness comparisons between R_A, R_B are determined exclusively by $\mathcal{E}(\cdot)$. \square

Property 3. If *EMSCO* solves (10), then it solves (6).

Proof. This result follows quickly from the construction of fitness⁶. Any solution that globally maximizes fitness will be necessarily be non-dominated. \square

EMSCO aims to respect both aggregated, scalarized performance ($\mathcal{E}(\cdot)$) and non-domination level/rank. Unlike algorithms such as NSGA-II (Deb et al., 2002), initial fitness is not determined exclusively by non-domination level, and only the *unique* chromosomes in the first non-dominated front (E_0^*) are carried to the next generation automatically. The remaining slots in the subsequent population are filled by executing selection, recombination, and mutation on the entire population in a manner that is biased against but does not exclude low-rank solutions. In our context, low ranked solutions may provide utility under the raw scalarized perspective (high $\mathcal{E}(\cdot)$) and/or be in proximity to high-performing in terms of genetic distance. As a cursory demonstration, Figure 6 depicts the volatility of the solution space near a non-dominated chromosome with respect to genetic distance. Blue vectors map to chromosomes within the n -dimensional *von Neumann Neighborhood* (Weisstein, 2012) of the red point’s corresponding chromosome. This performance landscape is computed on the Australian Credit Approval data set with chromosomes in $\mathcal{S}_{(14,4)}$ (Section 4.2).

4 Experiments

To evaluate *EMSCO*’s capabilities, experiments are conducted on three data sets from the UCI Machine Learning Repository (Dua and Graff, 2017) and one synthetic data set. To gauge performance under a variety of conditions, several confidence thresholds and feature cost schemes are considered. Experiments in Section 4.3 empirically evaluate *EMSCO*’s capacity for global optimization, and experiments in Section 4.4 compare *EMSCO* with various classification protocols—both traditional and budgeted approaches.

⁶Note that this result holds for any scalarization that is increasing with respect to all g_1, g_2, g_3 (Boyd and Vandenberghe, 2004).

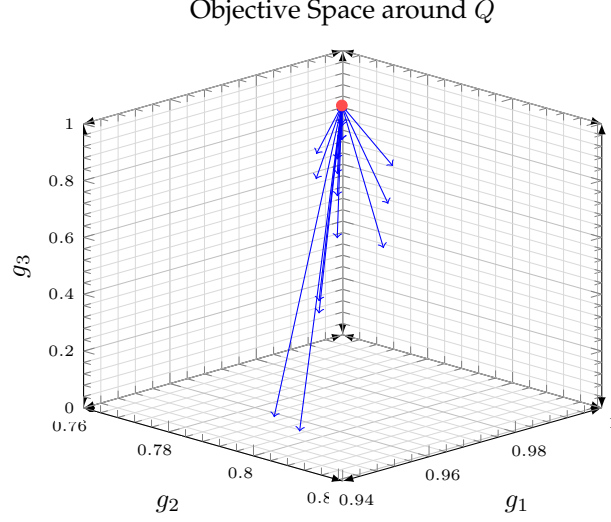


Figure 6: The performance landscape of chromosomes within one unit of $[Q]$ (red). A single ± 1 modification in $[Q]$ may have significant consequences for performance. In this figure, inverse cost is computed globally: $g_3 = \frac{\min_{U \in \mathcal{S}(n,k)} g_3^*(U)}{g_3^*(Q)}$

4.1 Parameter Tuning

EMSCO's parameters are tuned independently for each data set on training/validation splits with a simple "sweep" method (De Jong, 2007). Population size ($\|G\|$), mutation rate (\hat{m}), recombination rate (\hat{r}), elite percent threshold (b), and the mutation bias parameter (β) are subject to tuning. Continuous parameters ($\hat{m}, \hat{r}, b, \beta$) are discretized within an appropriate range, and all possible combinations of parameters in these ranges are tested. To evaluate performance of a particular combination of parameters, EMSO is run ten times using the given parameters with convergence settings fixed ($g = 20$ and $max_iter = 100$) and $k = \lceil \frac{n}{2} \rceil$. The following score is averaged over the ten runs to measure performance of each parameter combination:

$$\mathcal{E}^* = \ell_2 \left(g_1(Q_{max}), g_2(Q_{max}), \frac{1}{\log g_3^*(Q_{max})} \right),$$

where Q_{max} denotes the top-ranked chromosome in the final population. The third element, $\frac{1}{\log g_3^*(Q_{max})}$, is used to measure inverse cost in an absolute sense. When ranking performance of parameter combinations, we apply the following protocol during sort. If two parameter combinations have scores $\mathcal{E}_1^*, \mathcal{E}_2^*$ such that $|\mathcal{E}_1^* - \mathcal{E}_2^*| < \delta$, for some $\delta > 0$, population size is used as a tie-breaker. Lower population size is preferred for computational efficiency. If the two solutions have equal population size, the original ordering is maintained. For experiments, we set $\delta = .025$.

| Parameter | Tested Values |
|-----------|-----------------------------|
| \hat{m} | $[0.025, 0.1]_{0.025}$ |
| \hat{r} | $[0.70, 0.90]_{0.05}$ |
| β | $[2.0, 3.0]_{0.5}$ |
| b | $[0.1, 0.3]_{0.1}$ |
| $\ G\ $ | $\{200, \dots, 400\}_{100}$ |

Table 2: Parameter Tuning Domain

See Table 2 for the tested parameter ranges. The subscript in each entry is used to denote the size of gaps between elements. These ranges and increments are chosen to encompass a suitable breadth of parameter choices under the constraint of maintaining computational tractability—in our setup, tuning is an expensive procedure. Up to 100 generations must be created and evaluated for each parameter combination (up to 1000 generations for each of the 10 trials). While this tuning procedure is not exhaustive, EMSCO is generally robust as parameters vary in these experiments (Figure 7), and more rigorous tuning should only improve performance of EMSCO. Note, confidence threshold \hat{p} is not subject to tuning as the method assumes that conclusiveness requirements are fixed *a priori*.

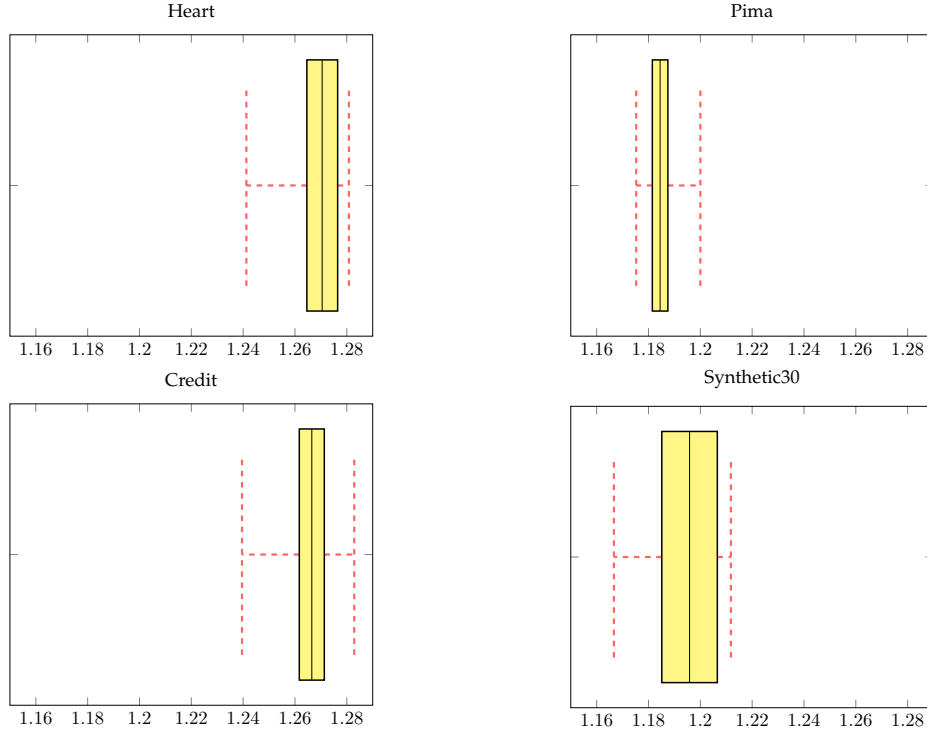


Figure 7: Range of $\mathcal{E}^*(Q_{max})$ as parameters vary in Table 2 on a validation set. The yellow region depicts the interquartile range and red lines correspond to minimum/maximum values of $\mathcal{E}^*(Q_{max})$ for all parameter combinations on the respective data set.

4.2 Data Sets

Each data set’s features, costs, and respective EA parameters are detailed in this section. The feature costs are assigned with various scaling functions dependent on their assigned *cost class*, which is an integer value associated with the time/cost required to acquire the respective feature. Data sets are chosen to represent pathologies (missing data, mixture of categorical and continuous variables, etc.) occurring frequently in real data.

4.2.1 Heart Failure Clinical Records

The Heart Failure Clinical Records data set is available on the UCI Machine Learning Repository and was compiled from 299 patients (Chicco and Jurman, 2020). As seen in Table 3, the data set consists of 12 pertinent clinical features that are a mix of categorical, integer, and real values. With the guidance of the data set’s author, time classes were assigned to each feature representing the acquisition cost. Features that can be acquired without running a test or a follow-up appointment are assigned time class ‘1’, otherwise, the feature is assigned to time class ‘2’. For this data set, the cost-scaling function is set as $h(T_i) = 10^{T_i}$, where T_i denotes the cost class of the i th feature. See Table 3 for a description of the features, their cost classes, and the EA parameters used in experiments. Note, we refer to this data set as “Heart” for the duration of this paper.

| Feature | Cost | Description |
|--------------------|------|--------------------------------|
| \mathcal{F}_1 | 1 | Age of Patient |
| \mathcal{F}_2 | 2 | Anaemia: {0,1} |
| \mathcal{F}_3 | 2 | High Blood Pressure: {0,1} |
| \mathcal{F}_4 | 2 | Creatinine Phosphokinase Level |
| \mathcal{F}_5 | 2 | Diabetes: {0,1} |
| \mathcal{F}_6 | 2 | Ejection Fraction |
| \mathcal{F}_7 | 2 | Platelets |
| \mathcal{F}_8 | 1 | Sex: {0,1} |
| \mathcal{F}_9 | 2 | Serum Creatinine |
| \mathcal{F}_{10} | 2 | Serum Sodium |
| \mathcal{F}_{11} | 1 | Smoking: {0,1} |
| \mathcal{F}_{12} | 1 | Follow-Up Period |
| Target | N/A | Death Event: {0,1} |

| Parameter | Value | Description |
|-----------|-------|--------------------------|
| \hat{m} | 0.075 | Mutation Rate |
| \hat{r} | 0.75 | Crossover Rate |
| b | 0.2 | Elite Population Percent |
| $\ G\ $ | 300 | Population Size |
| β | 2 | Mutation Bias Parameter |
| \hat{p} | 0.75 | Confidence Threshold |

Table 3: Heart Failure Clinical Records Features and Parameters

4.2.2 Pima Diabetes Data Set

The Pima Diabetes Data Set (Dua and Graff, 2017) is a popular data set for evaluating performance of classification models. An array of both integer and real-valued features are used to predict whether or not the patient will be diagnosed with diabetes. To evaluate performance of EMSCO on feature sets with multiple cost classes, values $T_i \in \{1, 2, 3\}$ were assigned to each

feature depending on the time and complications inherent in conducting the individual tests. For this data set, we use the linear scaling function $h(T_i) = 100T_i$. See Table 4 for a description of the features and their corresponding cost classes. Note, we refer to this data set as “Pima” for the remainder of this paper.

| Feature | Cost | Description |
|-----------------|------|-------------------------------|
| \mathcal{F}_1 | 1 | Number of times pregnant |
| \mathcal{F}_2 | 3 | Plasma glucose concentration |
| \mathcal{F}_3 | 2 | Diastolic blood pressure |
| \mathcal{F}_4 | 2 | Triceps skin fold thickness |
| \mathcal{F}_5 | 3 | 2-Hour serum insulin |
| \mathcal{F}_6 | 2 | Body mass index |
| \mathcal{F}_7 | 2 | Diabetes pedigree function |
| \mathcal{F}_8 | 1 | Age |
| Target | N/A | Diabetes diagnosis: $\{0,1\}$ |

| Parameter | Value | Description |
|-----------|-------|--------------------------|
| \hat{m} | 0.075 | Mutation Rate |
| \hat{r} | 0.8 | Crossover Rate |
| b | 0.20 | Elite Population Percent |
| $\ G\ $ | 300 | Population Size |
| β | 2 | Mutation Bias Parameter |
| \hat{p} | 0.65 | Confidence Threshold |

Table 4: Pima Diabetes Data Set Features and Parameters

4.2.3 Synthetic30 Data Set

The Synthetic30 dataset was constructed using `sklearn’s make_classification()` function (Pedregosa et al., 2011). The data set consists of 30 features and 1000 records. To address multi-class settings, three labels are assigned to the records proportionally.

To mimic scenarios in which a fraction of features are not discriminative for classification (Trapeznikov et al., 2013), the parameter `n_important` in `make_classification()` was set to 25. Gini impurity reduction (Scornet, 2020) is used to rank features in terms of importance and thereafter assign cost classes to each feature. Five such cost classes are used, where the most important features are placed in the highest cost class. Let x_i denote the percentile of the i th feature’s importance in terms of Gini impurity reduction. Cost class, $T_i \in \{1, 2, \dots, 5\}$, is defined as follows:

$$T_i = \begin{cases} 1 & 0 \leq x_i \leq .2 \\ 2 & .2 < x_i \leq .4 \\ 3 & .4 < x_i \leq .6 \\ 4 & .6 < x_i \leq .8 \\ 5 & .8 < x_i \leq 1.0 \end{cases}$$

Final cost of the i th feature is a linear function of its cost class: $h(T_i) = 100T_i$. This data set is referred to as “Synthetic30” for the rest of the paper.

| Parameter | Value | Description |
|-----------|-------|--------------------------|
| \hat{m} | 0.05 | Mutation Rate |
| \hat{r} | 0.8 | Crossover Rate |
| b | 0.20 | Elite Population Percent |
| $\ G\ $ | 300 | Population Size |
| β | 2.5 | Mutation Bias Parameter |
| \hat{p} | 0.65 | Confidence Threshold |

Table 5: Synthetic30 Diabetes Data Set Parameters

4.2.4 Australian Credit Approval Data Set

This data set is available on the UCI Machine Learning Repository (Quinlan, 1987) and consists of 14 features given in credit applications to a large bank. The target for this data set is binary. Feature descriptions are not provided given the sensitive nature of the data, but the values are designated as continuous or categorical. This data set contains missing values.

Three cost classes are assigned to the features according to their mean decrease in impurity (Gini importance), where features of greater importance are assigned greater cost classes. For this data set, the cost-scaling function is set as $h(T_i) = 10^{T_i}$. This data set is referred to as "Credit" in this paper.

| Feature | Cost | Description |
|--------------------|------|-----------------------|
| \mathcal{F}_1 | 2 | Categorical: {0,1} |
| \mathcal{F}_2 | 2 | Continuous |
| \mathcal{F}_3 | 2 | Continuous |
| \mathcal{F}_4 | 1 | Categorical: {1,2,3} |
| \mathcal{F}_5 | 2 | Categorical: {1...14} |
| \mathcal{F}_6 | 1 | Categorical: {1...9} |
| \mathcal{F}_7 | 2 | Continuous |
| \mathcal{F}_8 | 3 | Categorical: {0,1} |
| \mathcal{F}_9 | 1 | Categorical: {0,1} |
| \mathcal{F}_{10} | 2 | Continuous |
| \mathcal{F}_{11} | 1 | Categorical: {0,1} |
| \mathcal{F}_{12} | 1 | Categorical: {1,2,3} |
| \mathcal{F}_{13} | 1 | Continuous |
| \mathcal{F}_{14} | 2 | Continuous |
| Target | N/A | Class {0,1} |

| Parameter | Value | Description |
|-----------|-------|--------------------------|
| \hat{m} | 0.075 | Mutation Rate |
| \hat{r} | 0.80 | Crossover Rate |
| b | 0.20 | Elite Population Percent |
| $\ G\ $ | 300 | Population Size |
| β | 2.5 | Mutation Bias Parameter |
| \hat{p} | 0.75 | Confidence Threshold |

Table 6: Australian Credit Data Set Features and Parameters

4.3 Global Optima Experiment

In these experiments, EMSCO's global optimization abilities are tested. The object is to show that EMSCO can *quickly* find and maintain multiple globally non-dominated solutions.

To establish the true Pareto front for a particular data set in a k -stage solution space, a brute-force evaluation of all chromosomes in $\mathcal{S}_{(n,k)}$ is necessary. This endeavor presents a great computational burden and took roughly one month on a 32-core compute server to complete for all data sets. The largest experiment (Australian Credit data set: $n = 14, k = 4$) required evaluation of over 250 million solutions to establish the global Pareto front. Each solution was evaluated by training its respective k stages (subclassifiers) and recording performance of the corresponding multi-stage system on a test set that is assumed to capture the input space \mathcal{X} . To reduce runtime, each data set’s 2^n possible subclassifiers were trained and cached for fast evaluation. Despite such measures, the Synthetic30 data set could not be included in these experiments due to excessive computational expense.

After establishing the global Pareto front for each data set and stage-count ($k = 2 \dots 4$), EMSCO was run one-hundred times, and the average count of unique Pareto optimal solutions present in each h th elite population (\bar{X}_h) was recorded. Let μ_h denote the true mean number of unique Pareto optimal solutions in EMSCO’s h th elite population. 95% confidence intervals for μ_h are constructed at each generation and depicted in the second column of Figure 8. Note, due to time-constraints, we conducted experiments with $max_iter = 150$. If halting conditions (ii) or (iii) were triggered during iteration at generation G_h , then we copied X_h to subsequent generations’ counts. While 150 generations proved sufficient to demonstrate EMSCO’s capacity for quickly finding and maintaining a considerable number of globally optimal chromosomes (the primary purpose of this experiment), there are several plots that do not indicate the maximum number of globally non-dominated solutions EMSCO could possibly find if given more generations. For instance, \bar{X}_h is steadily increasing at the 150th generation in the Credit $k = 3$ plot.

In all experiments, EMSCO consistently obtained numerous Pareto optimal solutions while requiring at most 25 minutes of CPU-time to reach the 150th generation in our computing environment. Property 1 is manifest in each chart—all curves are monotonic. Nonetheless, experiments suggest that Property 1 does not necessarily preclude a wide breadth of search—in several experiments, a majority fraction of the entire global frontier was found and maintained in EMSCO’s elite population by the 150th generation. Table 7 lists the size of each global frontier. Relative to the size of their respective solution spaces, the frontiers are remarkably small.

Consider, for example, the corresponding search space of the Credit $k = 4$ experiment—only 171 of roughly 250 million chromosomes are globally non-dominated. Nevertheless, within minutes (150 generations), EMSCO effectively traversed the solution space to identify and maintain over 10% of the global frontier, on average. It is uncertain what fraction of the global Pareto frontier would be identified by EMSCO in later generations; However, the positive tangent at the terminal generation suggests an increase.

The Heart ($\mathcal{S}_{(12,4)}$) solution space is quite large with more than 15 million chromosomes; However, its Pareto frontier is very small, with only 33 solutions. In the corresponding experiment, EMSCO again demonstrates its ability to quickly traverse a vast solution space with a sparse Pareto frontier and find/maintain a considerable fraction of unique globally non-dominated solutions—in this case, almost two-thirds of the global frontier in less than 150 generations.

| Data Set | k=2 | k=3 | k=4 |
|----------|-----|-----|-----|
| Heart | 24 | 28 | 33 |
| Credit | 47 | 141 | 171 |
| Pima | 18 | 42 | 65 |

Table 7: Global Pareto Frontier Sizes

4.4 Comparison Against Alternative Budgeted Methods

These experiments evaluate the performance of EMSCO against two popular budgeted classification methods, a cost-ordered n -stage classifier, and a traditional single-stage classifier. The classifier *evaluation* cost is set as zero for all methods and data sets, since evaluation at each stage is negligible for the moderately-sized data sets used in these experiments.

Greedy Miser (Xu et al., 2012) is a variant of stage-wise regression (Friedman, 2001) with a feature-budgeted loss function. In this method, regression trees are added iteratively to form a feature-budgeted ensemble classifier. To evaluate this method in our setup and compute coverage rates, we incorporate a reject option before label assignment that discards low-confidence predictions under the given threshold (\hat{p}). Because of this modification, we denote this method as GM*

Cost-Sensitive Tree of Classifiers (Xu et al., 2014) builds a tree of classifiers optimized for a specific sub-partition of the input space. The aim is to ensure that inputs are classified using only the most pertinent features defined for particular regions of the input space. Doing so reduces unnecessary feature extraction while maintaining accuracy. As with Greedy Miser, we add a reject option to this method that discards predictions below a given threshold. Because of this modification, we denote this method as CSTC*

The n -stage classifier is considered as a simple heuristic that utilizes a common *cost-ordered* perspective for ordering features in budgeted systems (Trapeznikov et al., 2013; Wang et al., 2014). A traditional single-stage classifier with no terminal reject option (100% coverage) is included to benchmark against out-of-box methods. The n -stage and single-stage methods both apply logistic regression at each stage to classify inputs.

Note, we consider Greedy Miser and CSTC because they are among the best-cited budgeted learning approaches, have code available online, and can be easily modified to apply confidence-based reject decisions; However, it is important to note that Greedy Miser and CSTC are optimized with respect to traditional accuracy—not “conclusive accuracy” as it is defined in this manuscript. We also assume that these methods are sufficiently well-calibrated (Kull et al., 2017) such that their confidence scores roughly approximate true class probabilities as in logistic regression—the classification algorithm utilized by EMSCO at each stage. These factors can inflate conclusive accuracy and decrease coverage when the reject protocol is applied (if confidence scores are conservative), but cost is not influenced. To the best of our knowledge, there is not another budgeted method with a terminal reject option considering accuracy, feature acquisition cost, and coverage simultaneously. Current methods must therefore be adapted to fit this paper’s setup in experiments.

4.4.1 Performance Evaluation

To train, tune, and evaluate methods, a 50-25-25 training, validation, and testing split is used for each data set. For a given chromosome Q , EMSCO uses the training set to learn its subclassifiers ($\mathcal{C}(Q_j)$) comprising each j^{th} stage. Each experiment conducts fifty independent trials—EMSCO is run on the validation set with the parameters listed in Section 4.2 and $\text{max_iter} = 150$, $g = 20$, $k = \lceil \frac{n}{2} \rceil$. At each terminal generation, the chromosome with maximum fitness is stored.

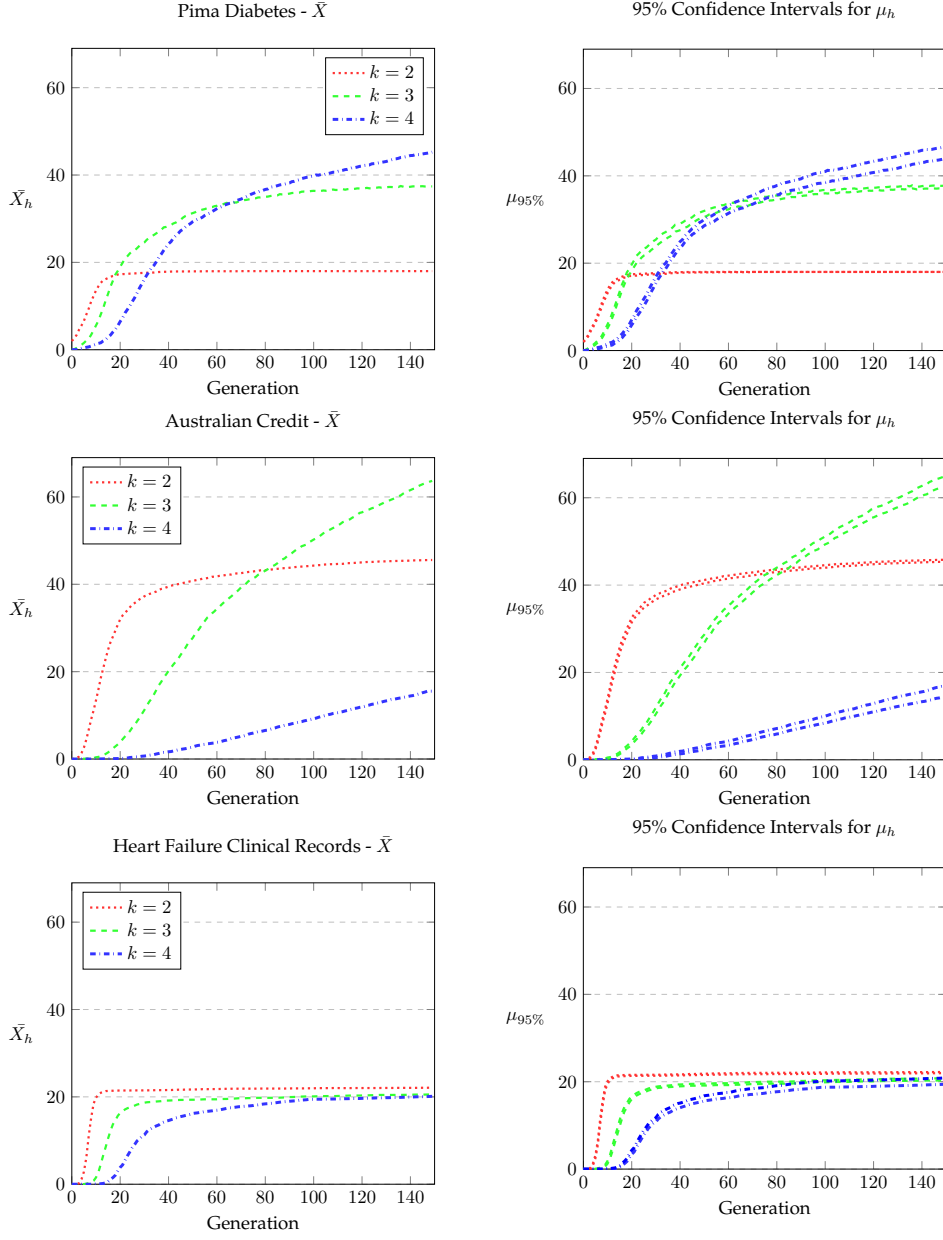


Figure 8: Column (a): \bar{X}_h denotes the sample mean (100 samples) for the count of unique Pareto optimal solutions present in EMSCO's h th generation. Column (b): The upper and lower bounds of the 95% confidence interval for μ_h , the true mean count of optimal solutions in G_h .

When the experiment is finished, these fifty chromosomes are used to compute average g_1, g_2, g_3^* values *on the test set* (50 samples), marking EMSCO’s performance. Since inverse cost (g_3) is population-dependent, *raw* cost (g_3^* as defined in Section 2.2.3) is displayed for each method in these experiments. Due to the stochastic nature of evolutionary algorithms, a 95% margin of error value (ϵ_{EA}) is included in each chart (Figures 9-12).

The alternative methods were evaluated by tuning parameters on a validation set and then recording performance on the testing set. As done in (Xu et al., 2012) and (Xu et al., 2014) GM* and CSTC*’s parameters were tuned using grid search on a large discretized set of choices. These alternative methods are deterministic, and margin of error is not computed.

4.4.2 Results

In the Pima comparison experiment, EMSCO exhibits strong performance with lowest cost (80% lower than a traditional single stage classifier), and highest coverage among all budgeted methods. Although EMSCO’s accuracy on this data set is similar to a single-stage classifier, it is lower than the other budgeted methods. However, since a 65% confidence threshold was applied, it could be argued that conclusive accuracy of 70.1% is sufficient given the system monitor’s expectations. In comparison, CSTC* and GM* yielded a higher accuracy that may be preferable in certain instances if very low conclusiveness and higher cost are acceptable.

For the Credit dataset, EMSCO again reported the lowest cost among all tested methods (79% lower than a traditional single-stage classifier), and second highest conclusiveness among budgeted protocols. With respect to accuracy, EMSCO offered good performance (82% conclusive accuracy). GreedyMiser showed relatively low conclusiveness and highly inflated cost. As in the Pima experiment, CSTC* had highest conclusive accuracy but low conclusiveness compared to alternatives.

GM* stands out in the Heart experiment for its strong performance across all objectives and minimal cost (81% less than a single-stage classifier and 65% less than CSTC*). However, conclusiveness is slightly low, ranking ahead of only one other method (CSTC*). CSTC* likewise provides remarkably high accuracy but only classifies about half of inputs. EMSCO provides strong accuracy (85.1%) the highest conclusiveness among budgeted approaches and exhibits a significant reduction in cost compared to n -Stage and traditional out-of-box logistic regression.

In the Synthetic30 experiment, EMSCO provides balanced performance with highest conclusiveness and accuracy among the budgeted methods. Furthermore, the cost for EMSCO is 62% less than a single-stage classifier. Note that EMSCO Pareto dominates CSTC* in this multi-class setting. GM* offers very low cost and high conclusiveness, but its conclusive accuracy (44.2%) is likely disqualifying given the system monitor’s desire to be correct in roughly 65% of instances.

In all experiments, EMSCO is non-dominated and exhibits balanced performance across objectives. EMSCO’s conclusive accuracy exceeded \hat{p} in every case, suggesting EMSCO’s confidence-based reject protocol was effective in maintaining accuracy above a specified minimum. In this paper’s setup, $g_2 \geq \hat{p}$ can be viewed as sufficient given the preferences of a risk-averse monitor (Section 2) applying the threshold. Indeed, a monitor with different preferences/misclassification penalties could adjust the confidence threshold to increase g_2 .

In 2 of 4 total experiments, EMSCO yielded the lowest average classification cost, and, in the other 2 experiments, was only outperformed in this metric by methods with markedly lower conclusiveness (e.g., Heart-CSTC*/GM*) or low accuracy (e.g., Synthetic30-GM). With regard to conclusiveness, EMSCO assigned labels to, on average, 93.4% of inputs—representing a utility loss of only 6.6% compared to a traditional non-selective method without a terminal reject option. EMSCO likewise offers a 475% average speed increase and an accuracy decrease of only 2.72% compared to a traditional approach that acquires all features for all inputs. GreedyMiser and CSTC* reported an average utility loss of 45.2% and 36.4%, respectively. Compared to

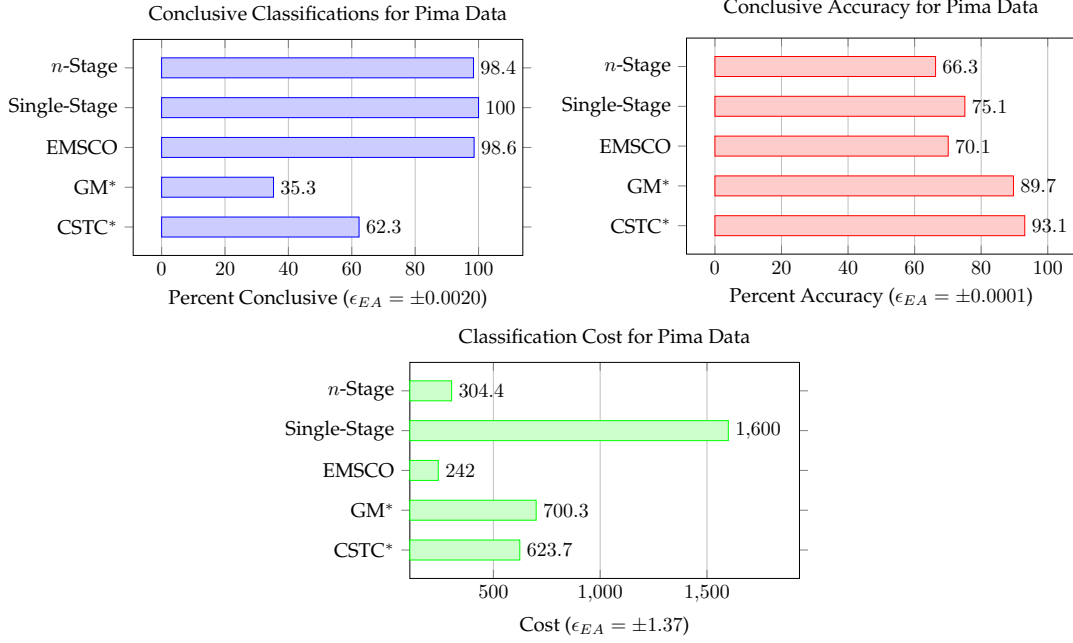


Figure 9: Comparison results for the Pima Diabetes Data Set.

n-Stage, EMSCO provided lower cost in each experiment—most notably in the Synthetic30 experiment—and achieved markedly higher accuracy. EMSCO also distinguished itself for its ability to handle multi-class data as shown in the Synthetic30 experiment, where GM* and CSTC* struggle to accurately classify inputs. Note that EMSCO’s accuracy is comparable to the traditional logistic regression model in all experiments, and accuracy could possibly be increased by incorporating a more sophisticated classification algorithm at each stage. Though, deploying an expensive classification algorithm at each stage could yield non-trivial classifier evaluation cost.

Figure 13 depicts the number of correct, accepted predictions provided by each method.

5 Conclusion

In this manuscript, EMSCO, an evolutionary algorithm for optimizing high-coverage, low-cost multi-stage classifiers, was proposed. This method was shown capable of effectively managing three important objectives and providing balanced performance. Compared to alternative approaches, EMSCO offered solutions with high coverage, low cost, and sufficient accuracy. Additionally, the method proved itself capable of identifying globally Pareto optimal solutions within very large solution spaces in multiple experimental settings. However, there are several limitations of EMSCO that should be noted.

Due to their heuristic nature, evolutionary algorithms do not provide guarantees of optimality. While the experiments in Figure 8 are encouraging, similar results cannot be ensured in the general case. It is particularly important to consider whether these patterns persist in the context of higher dimensional data, but the combinatorial burden imposed by our setup makes addressing this case difficult for very large n . Another downside to a population-based

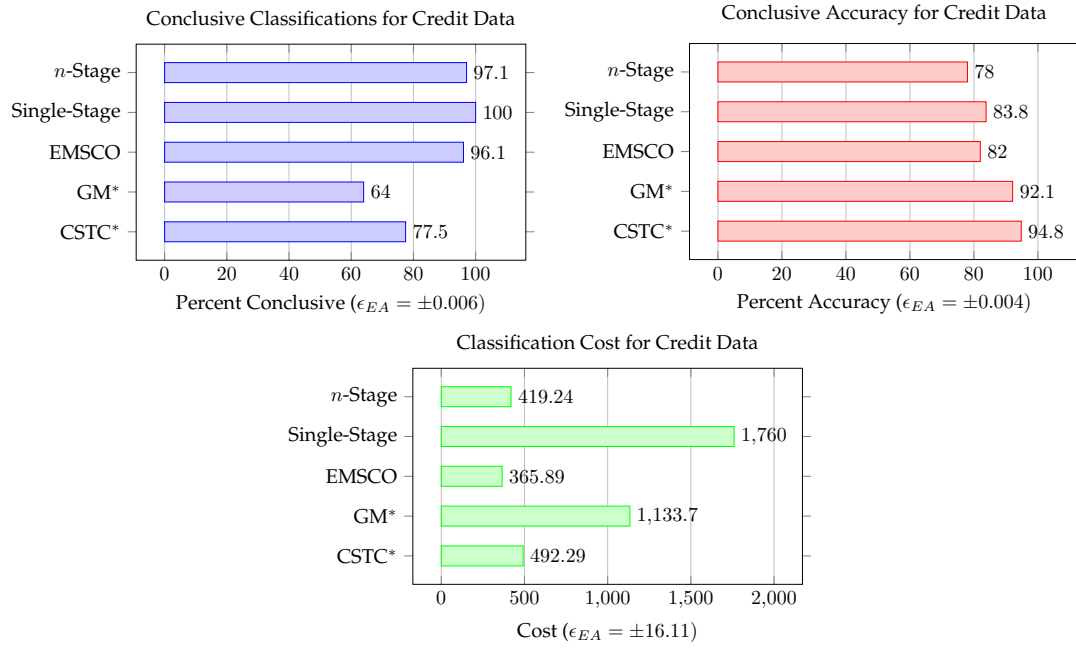


Figure 10: Comparison results for the Australian Credit Data Set.

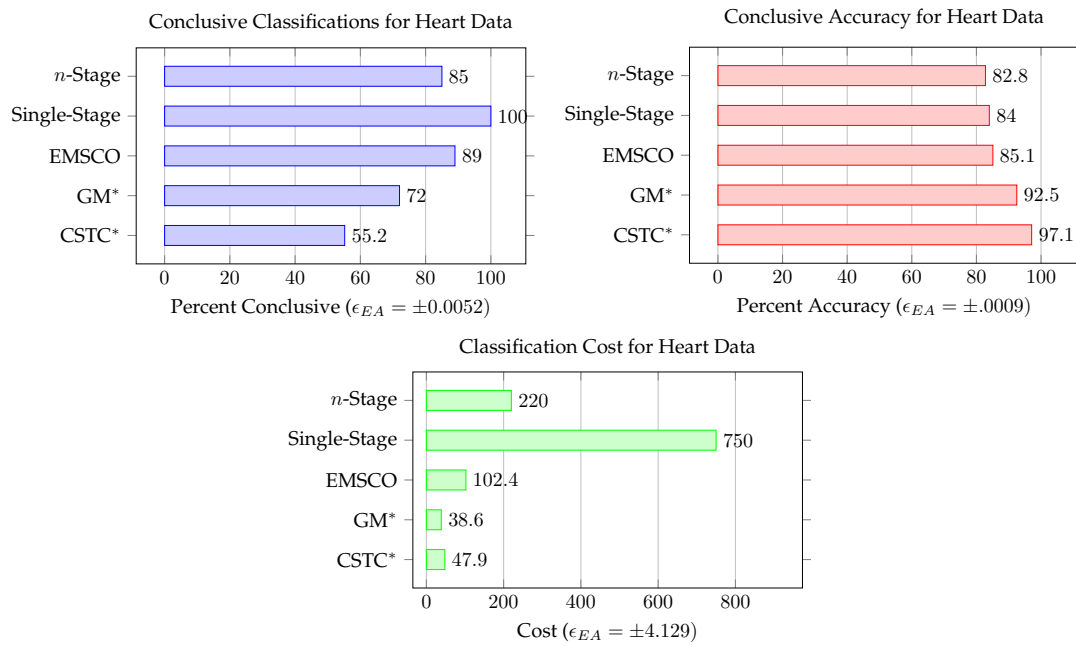


Figure 11: Comparison results for the Heart Failure Clinical Records dataset.

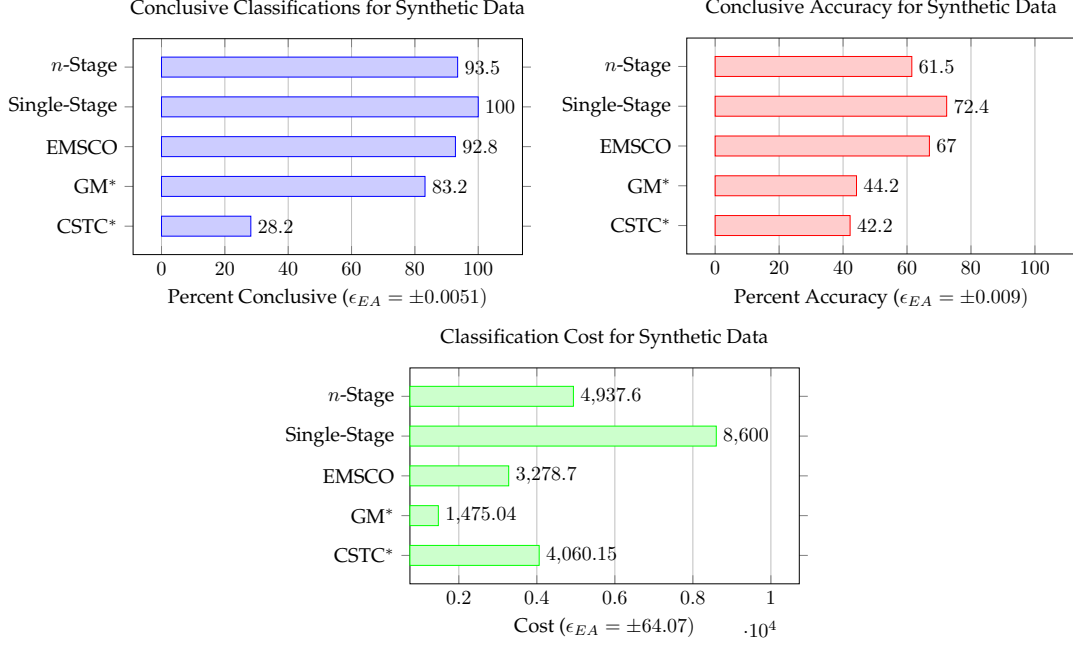


Figure 12: Comparison results for the synthetic30 dataset.

approach such as EMSCO involves training/validation time. Indeed, if $\mathcal{S}_{(n,k)}$ is very large (trillions of solutions), EMSCO could require many generations to converge depending on the fitness landscape.

5.1 Future Work

Feature Removal Option. To further reduce cost, future work may benefit from including a *feature removal option* in the chromosome representation. For example, the mutation operator could be modified to allow assignment $[Q]_i = -1$, representing removal of feature i from all stages. This protocol may prove particularly useful when n is large and feature selection can reduce complexity and cost (Yu et al., 2020).

New Objectives. The number and choice of objectives could also be modified. Currently, EMSCO optimizes with respect to three objectives, but these could be altered depending on the setting. Certain contexts impose severe penalties for false positives that may warrant explicit consideration of this value as an objective. In light of this, one potentially useful objective is inverse false-positive rate (FPR)—since EMSCO maximizes objectives in $[0, 1]$, the value $1 - \text{FPR}(Q)$ could be included as an objective to be maximized. Additionally, to bias the method towards low stage counts, an inverse stage count could be leveraged as an objective. This modification could replace or supplement the bias introduced during mutation (Section 3.2.3).

Enhanced Reject Decision. The current reject protocol (confidence thresholds) yields desired performance in experiments, is fast to compute, and intuitive; However, it is perhaps too simplistic for certain settings. Given that many real-world scenarios impose varying costs for false positives and false negatives (Zhou and Liu, 2006), future work may benefit from incorporating different confidence thresholds for positive and negative predictions. Likewise, for high k , where there are additional opportunities for marginal, incorrect predictions to be accepted,

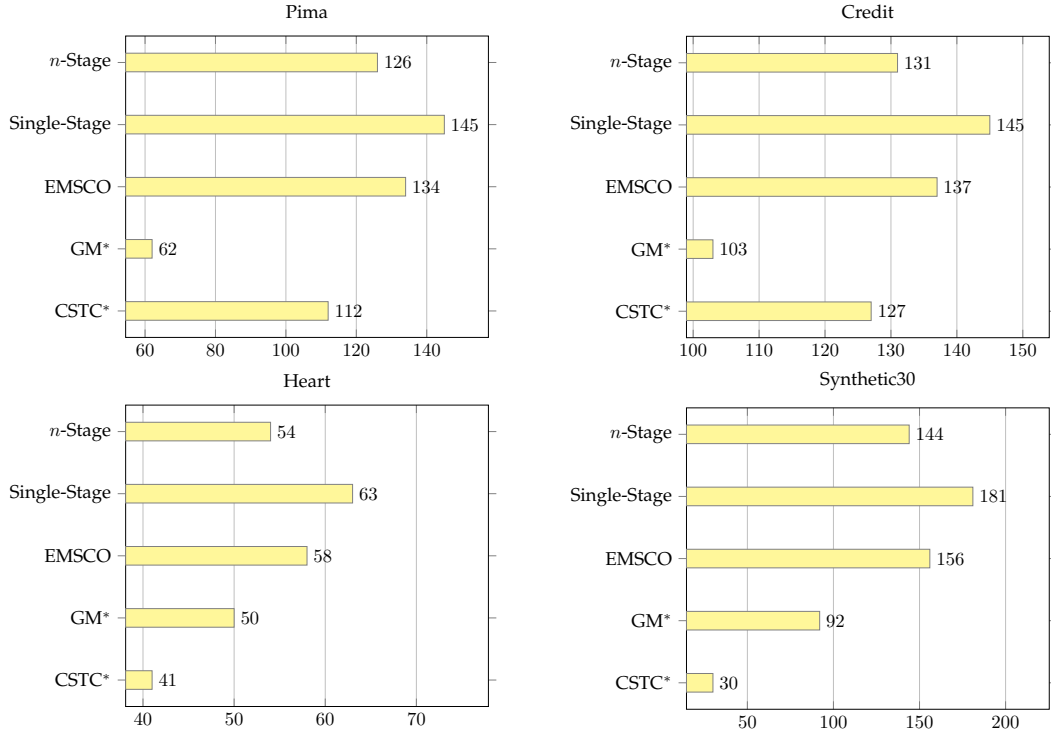


Figure 13: Number of correct, accepted predictions provided by each method. In all experiments, EMSCO provides the greatest number of correct, accepted predictions among budgeted methods while ensuring accuracy above \hat{p} .

the reject decision could be modified in an attempt to preserve accuracy at or above the initial specified level (\hat{p}) with higher probability.

References

- Artières, T., Contardo, G., and Denoyer, L. (2016). Recurrent neural networks for adaptive feature acquisition. *23rd International Conference on Neural Information Processing*.
- Boyd, S. and Vandenberghe, L. (2004). *Convex Optimization*. Cambridge University Press.
- Casella, G. and Berger, R. (2001). *Statistical Inference*. Duxbury Resource Center.
- Chicco, D. and Jurman, G. (2020). Heart failure clinical records data set. UCI Machine Learning Repository.
- Cortes, C., DeSalvo, G., and Mohri, M. (2016). Learning with rejection.
- De Jong, K. (2007). Parameter setting in eas: a 30 year perspective. In *Parameter setting in evolutionary algorithms*, pages 1–18. Springer.
- Deb, K. (2001). *Multi-Objective Optimization Using Evolutionary Algorithms*. John Wiley & Sons, Inc., New York, NY, USA.
- Deb, K., Pratap, A., Agarwal, S., and Meyarivan, T. (2002). A fast and elitist multiobjective genetic algorithm: Nsga-ii. *IEEE Transactions on Evolutionary Computation*, 6(2):182–197.

- Dua, D. and Graff, C. (2017). UCI machine learning repository.
- Dundar, M. M. and Bi, J. (2007). Joint optimization of cascaded classifiers for computer aided detection. In *2007 IEEE Conference on Computer Vision and Pattern Recognition*, pages 1–8.
- Eiben, A. and Smith, J. (2015). *Introduction to Evolutionary Computing*. Natural Computing Series. Springer. Gebeurtenis: 2nd edition.
- El-Yaniv, R. and Wiener, Y. (2010). On the foundations of noise-free selective classification. *Journal of Machine Learning Research*, 11(53):1605–1641.
- Friedman, J. H. (2001). Greedy function approximation: A gradient boosting machine. *The Annals of Statistics*, 29(5):1189 – 1232.
- Geifman, Y. and El-Yaniv, R. (2017). Selective classification for deep neural networks.
- Hamilton, N. H. and Fulp, E. W. (2020). An evolutionary approach for constructing multi-stage classifiers. In *Proceedings of the 2020 Genetic and Evolutionary Computation Conference Companion, GECCO '20*, page 1730–1738, New York, NY, USA. Association for Computing Machinery.
- Hamilton, N. H., McKinney, S., Allan, E., and Fulp, E. W. (2020). An efficient multi-stage approach for identifying domain shadowing. In *ICC 2020 - 2020 IEEE International Conference on Communications (ICC)*, pages 1–7.
- Janisch, J., Pevný, T., and Lisý, V. (2019). Classification with costly features as a sequential decision-making problem. *CoRR*, abs/1909.02564.
- Ji, S. and Carin, L. (2007). Cost-sensitive feature acquisition and classification. *Pattern Recogn.*, 40(5):1474–1485.
- Knuth, D. E. (1998). *The Art of Computer Programming, Volume 3: (2nd Ed.) Sorting and Searching*. Addison Wesley Longman Publishing Co., Inc., USA.
- Kuhn, M., Johnson, K., et al. (2013). *Applied predictive modeling*, volume 26. Springer.
- Kull, M., Filho, T. M. S., and Flach, P. (2017). Beyond sigmoids: How to obtain well-calibrated probabilities from binary classifiers with beta calibration. *Electronic Journal of Statistics*, 11(2):5052 – 5080.
- Kusner, M. J., Chen, W., Zhou, Q., Xu, Z., Weinberger, K. Q., and Chen, Y. (2014). Feature-cost sensitive learning with submodular trees of classifiers. In *Proceedings of the Twenty-Eighth AAAI Conference on Artificial Intelligence, AAAI'14*, page 1939–1945. AAAI Press.
- Lichtblau, D. and Stoean, C. (2019). Cancer diagnosis through a tandem of classifiers for digitized histopathological slides. *PLoS One*.
- Nan, F., Wang, J., and Saligrama, V. (2016). Pruning random forests for prediction on a budget. In *Advances in Neural Information Processing Systems 29: Annual Conference on Neural Information Processing Systems 2016, December 5-10, 2016, Barcelona, Spain*, pages 2334–2342.
- Nogueira, R., Yang, W., Cho, K., and Lin, J. (2019). Multi-stage document ranking with bert.

- Patel, B. N., Rosenberg, L. B., Willcox, G., Baltaxe, D., Lyons, M., Irvin, J. A., Rajpurkar, P., Amrhein, T. J., Gupta, R., Halabi, S. S., Langlotz, C., Lo, E., Mammarappallil, J. G., Mariano, A. J., Riley, G., Seekins, J., Shen, L., Zucker, E., and Lungren, M. P. (2019). Human-machine partnership with artificial intelligence for chest radiograph diagnosis. *NPJ Digital Medicine*, 2.
- Pedregosa, F., Varoquaux, G., Gramfort, A., Michel, V., Thirion, B., Grisel, O., Blondel, M., Prettenhofer, P., Weiss, R., Dubourg, V., et al. (2011). Scikit-learn: Machine learning in python. *Journal of machine learning research*, 12(Oct):2825–2830.
- Peter, S., Diego, F., Hamprecht, F. A., and Nadler, B. (2017). Cost efficient gradient boosting. In Guyon, I., Luxburg, U. V., Bengio, S., Wallach, H., Fergus, R., Vishwanathan, S., and Garnett, R., editors, *Advances in Neural Information Processing Systems*, volume 30. Curran Associates, Inc.
- Quinlan, J. R. (1987). Simplifying decision trees. *Int. J. Man-Mach. Stud.*, 27(3):221–234.
- Scornet, E. (2020). Trees, forests, and impurity-based variable importance.
- Trapeznikov, K., Saligrama, V., and Castañón, D. (2013). Multi-stage classifier design. *Machine Learning*, 92(2-3):479–502.
- Viola, P. A. and Jones, M. J. (2001). Rapid object detection using a boosted cascade of simple features. In *CVPR (1)*, pages 511–518. IEEE Computer Society.
- Wang, J., Trapeznikov, K., and Saligrama, V. (2014). An LP for Sequential Learning Under Budgets. volume 33 of *Proceedings of Machine Learning Research*, pages 987–995, Reykjavik, Iceland. PMLR.
- Weisstein, E. W. (2012). von neumann neighborhood. From MathWorld—A Wolfram Web Resource.
- Xu, Z., Weinberger, K., and Chapelle, O. (2012). The greedy miser: Learning under test-time budgets.
- Xu, Z. E., Kusner, M. J., Weinberger, K. Q., Chen, M., and Chapelle, O. (2014). Classifier cascades and trees for minimizing feature evaluation cost. *Journal of Machine Learning Research*, 15(62):2113–2144.
- Yu, G., Witten, D., and Bien, J. (2020). Controlling costs: Feature selection on a budget.
- Zhou, Z.-H. and Liu, X.-Y. (2006). Training cost-sensitive neural networks with methods addressing the class imbalance problem. *IEEE Transactions on Knowledge and Data Engineering*, 18(1):63–77.